

Nanosatellite Navigation with the WMM2005 Geomagnetic Field Model

Mohammad Nizam FILIPSKI, Ermira Junita ABDULLAH

*Department of Aerospace Engineering, Faculty of Engineering Universiti Putra Malaysia
43400 UPM Serdang, Selangor D.E., MALAYSIA
e-mail: nizam@eng.upm.edu.my*

Received 03.05.2005

Abstract

Most current space missions require accurate knowledge of the satellite attitude and orbital position. Here the navigation system design will focus on the use of only one sensor, a magnetometer. A nanosatellite is considered as it is a straightforward solution to reduce the cost of the mission and provide space emerging countries like Malaysia with access to space. Therefore, the development of innovative navigation algorithms is of foremost interest as it will allow us to use fewer and cheaper sensors. This paper describes a navigation concept applied to a nanosatellite equipped with only a magnetometer. It emphasizes the latest geomagnetic field model available and provides a brief overview of the magnetometers used in micro- and nanosatellites.

Key words: Nanosatellite, Geomagnetic field model, WMM2005 model, AMR magnetometer.

Introduction

The navigation of a satellite implies the determination and control of both the orbit and the attitude of the satellite. The control of the orbit is required to maintain the satellite on the desired trajectory for the entire duration of the mission. The control of the attitude is very mission dependent in terms of requirements and it is necessary to point or slew the satellite in space. In this paper we will focus on the attitude determination problem and how to estimate the attitude from the measurement of the geomagnetic field.

The types of sensors used for low-cost nanosatel-

lites and microsattellites are preferably commercial off-the-shelf (COTS) sensors, meaning that they are not specifically designed for space applications. Solid-state sensors, like microgyros or magnetoresistive magnetometers are favored for their small size and low cost. They have the double advantage of reducing the total weight of the satellite, which means it is cheaper to send into space, and has very low power requirements. As an example a comparison between current and past gyroscope characteristics is made in Table 1. Note that the drift increases as the size of the gyros is reduced. To compensate for this loss of accuracy the algorithms used to estimate the attitude must be more efficient.

Table 1. Comparison of gyro specifications per decade.

Gyro	MASS	SIZE (cm)	POWER (W)	DRIFT (deg/h)
1970s	17 kg	~ 28 x 30 x 33	~ 22	0.003
1980s	5 kg	~ 28 x 20 x 10	~ 18	0.01
2000s	< 30 g	1.5 x 1.5 x 3	~ 1	~ 10

Mission Design

A satellite is easily differentiated from other objects by its weight and by the type of trajectory it is following. A classification of satellites according to their mass is given in Table 2. The satellite chosen for this mission is a nanosatellite. It is generally agreed that this type of satellite weighs between 1 kg and 10 kg.

Table 2. Classification of satellites according to their mass (from *Surrey Satellite Technology*).

	SSTL Classification
Large	> 400 kg
Small	100 – 400 kg
Micro	10 – 100 kg
Nano	1 – 10 kg
Pico	0.1 – 1 kg

The main justification for choosing a nanosatellite is that the cost of sending something into space is proportional to its mass: between USD 5,000 and USD 50,000 per kilogram, depending on the launcher and if the satellite is sent as a primary or secondary payload.

The orbit required to validate our navigation system would be around 500 km of altitude, circular, with an inclination of nearly 2 degrees. The orbital plane is therefore close to the equatorial plane. This

type of orbit is of particular interest to equatorial countries for remote sensing purposes.

For a given satellite the design of the attitude determination system depends on the attitude accuracy required to achieve the mission objectives. The requirement that we would like to achieve is an accuracy of better than 5° (3σ) about each axis of the satellite. As stated earlier we will limit the attitude determination hardware to a minimum to abide with the constraints of the low cost and small size of the satellite. The small size implies that the available power is limited by the reduced area of the solar panels, which are usually placed on the satellite sides, and also by the smaller battery carried by the satellite.

Earth’s Magnetic Field

The present knowledge states that the Earth’s magnetic field is a vector quantity depending on both space and time and made up of a superposition of 3 main sources, namely:

- the field generated by the Earth’s outer core, usually called the main field (\mathbf{B}_m)
- the field generated by the Earth’s crust and upper mantle regions, or lithosphere (\mathbf{B}_l)
- the field generated by ionospheric and magnetospheric electric currents (\mathbf{B}_c)



Figure 1. Satellite ground track in the geocentric inertial frame.

The total magnetic field above the Earth's surface is then written as

$$\mathbf{B}(\mathbf{r}, t) = \mathbf{B}_m(\mathbf{r}, t) + \mathbf{B}_i(\mathbf{r}, t) + \mathbf{B}_c(\mathbf{r}, t) \quad (1)$$

According to McLean (2004), the term \mathbf{B}_m contributes to over 95% of the total field.

The direction and intensity of \mathbf{B} are dependent of our observation point around the Earth as shown in Figure 2.

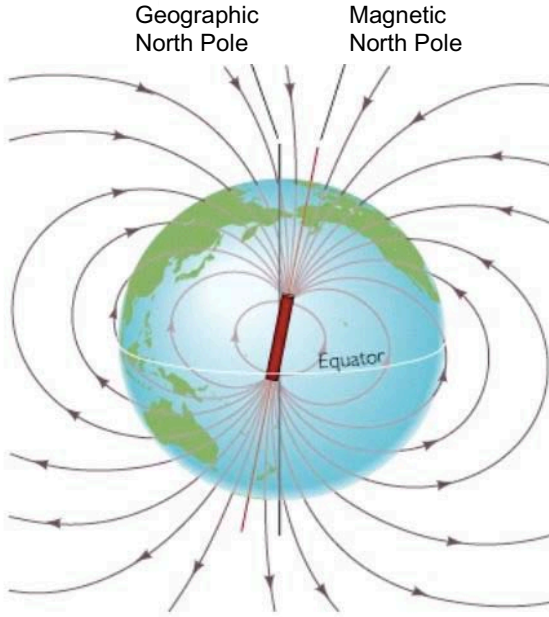


Figure 2. Earth's magnetic field lines.

The intensity of \mathbf{B} decreases with altitude and above 6000 km it is practically impossible to use the geomagnetic field to determine the satellite attitude. This is partly due to the influence of the term \mathbf{B}_c in Eq. (1). This term is not included in the common geomagnetic model like the one discussed in the next paragraph. At the Earth's surface the intensity of the field varies from approximately 50,000 nT (or 0.5 G) at the poles to 30,000 nT (or 0.3 G) at the equator. Above 10,000 km it becomes less than 2000 nT. The geomagnetic field resembles the field created by a bar magnet placed at the center of the Earth and having an inclination of approximately 10.5 degrees to the Earth's rotation axis. The intensity of the Earth's magnetic field is in reality quite irregular in spite of the general symmetry indicated in Figure 2. Indeed the field intensity slowly varies at different rates according to the position at the Earth's surface.

Earth Magnetic Modeling and WMM2005

Because the Earth's magnetic field is constantly changing with time it is necessary to develop a mathematical model to predict its future, or past, behavior. The derivation of the model requires the availability of measurement data and the better the quality of the data obtained the better the accuracy of the model. Measurements mainly come from satellites orbiting the Earth at low altitudes with the specific mission of gathering these data and also from ground observatories scattered across the Earth's surface. Orsted and Champ are satellites having flown this kind of mission and their data are used to produce the model we will discuss here. These 2 categories of data (ground and space) are complementary to each other: satellite data provide a good spatial coverage but are available sparsely in time, whereas data from observatories are available almost continuously but only at a limited number of positions.

The 2 main models used for practical applications are the International Geomagnetic Reference Field (IGRF) from the International Association for Geomagnetism and Aeronomy (IAGA) and the World Magnetic Model (WMM) developed by the US National Oceanic and Atmospheric Administration (NOAA) and the British Geological Survey (BGS). The WMM is the standard model used in military and civilian navigation systems in both the US and UK. The IGRF is the model preferred by the academic community and results from a voluntary effort made by a number of modeling teams associated with the IAGA (Macmillan, 2005). Both these models are revised at least every 5 years and are usually valid for 5 more years after their release. The latest models were issued in December 2004. Their denomination is WMM2005 and IGRF-10.

The different terms in the total field of Eq. (1) are usually modeled separately in the form of gradient of scalar potentials. The assumption is usually made that the geomagnetic field is irrotational in the area of interest so that we can write the vector field as the gradient of a potential function:

$$\mathbf{B}(r, \lambda, \theta, t) = -\nabla V(r, \lambda, \theta, t) \quad (2)$$

where (r, λ, θ) represent respectively the radius, the longitude and the co-latitude in a spherical, geocentric reference frame.

The mathematical model of the Earth's magnetic field originates from the solution of Eq. (2), where the potential V satisfies the Laplace equation since the divergence of \mathbf{B} is null,

$$\nabla^2 V(r, \lambda, \theta, t) = 0 \quad (3)$$

The general solution to this equation can be written as the sum of 2 series (Eq. (4)). One series of terms is r^n , which means that we are approaching the source when r increases and that the terms represent external field contributions. The other series of terms, $(1/r)^n$, becomes larger when r decreases. They represent the contribution of the Earth's internal fields.

$$V(r, \lambda, \theta, t) = a \sum_{n=1}^{\infty} \left[\left(\frac{r}{a}\right)^n S_n^e(\lambda, \theta) + \left(\frac{a}{r}\right)^{n+1} S_n^i(\lambda, \theta) \right] \quad (4)$$

where a is the standard Earth's magnetic reference radius (6371.2 km), S_n is the spherical harmonics function of the longitude λ and of the geocentric co-latitude θ . The superscript e stands for *external* and the superscript i for *internal*.

In practice the contributions of the external sources are minimal and not taken into account for most applications. Indeed the series is not included in the WMM or IGRF models. Olsen (2002) can be consulted for the parameterization of the external fields.

The spherical harmonics function $S_n(\lambda, \theta)$ can be written as the product of 2 variable-independent functions: one function of λ : $\cos(m\lambda)$ and $\sin(m\lambda)$, and one function of θ that is called associated Legendre polynomials $P_n^m(\cos\theta)$.

Considering this fact and using only the terms of the internal sources of Eq. (4), the potential can be written as

$$V(r, \lambda, \theta, t) = \sum_{n=1}^N \sum_{m=0}^n V_n^m = \quad (5)$$

$$a \sum_{n=1}^N \left(\frac{a}{r}\right)^{n+1} \sum_{m=0}^n (g_n^m(t) \cos(m\lambda) + h_n^m(t) \sin(m\lambda)) \tilde{P}_n^m(\cos\theta)$$

where $g_n^m(t)$ and $h_n^m(t)$ are the time-dependent Gauss coefficients of degree n and order m , and $\tilde{P}_n^m(\cos\theta)$

are the Schmidt normalized associated Legendre polynomials. Note that if the latitude is used instead of the co-latitude in the expression of the potential then $\cos\theta$ is replaced by the sinus of the latitude. For the purpose of modeling, the degree of the series is limited to N , which equals 12 for the WMM2005 model and 13 for the IGRF-10 model. The reasons for this limitation can be found in Campbell (2003) (p.31).

The time dependence of the geomagnetic field in Eq. (2) is modeled by the time dependence of the Gauss coefficients. Their variation with time is usually assumed to be linear for the 5-year validity period of the models. They are calculated from the following relations at the date t expressed in years,

$$g_n^m(t) = g_n^m + \dot{g}_n^m \times (t - t_0) \quad t_0 \leq t \leq t_0 + 5 \quad (6)$$

$$h_n^m(t) = h_n^m + \dot{h}_n^m \times (t - t_0) \quad t_0 \leq t \leq t_0 + 5 \quad (7)$$

where g_n^m and h_n^m are the main field coefficients at the reference date t_0 of the model (2005 for the WMM2005), \dot{g}_n^m and \dot{h}_n^m are the secular variation (SV) coefficients for the 5-year period following the reference date. It is these coefficients that describe a model and they are freely available in the form of a text file from the internet. The coefficients of the WMM2005 are given in Table 3.

In satellite navigation the geomagnetic field model is used for 2 different purposes. The most obvious and the one that comes to mind immediately is when the model is stored in the navigation system memory. Then it is used in such a way that the real value of the geomagnetic field, measured by onboard instrumentations, is compared to the value given by the model. The result of this comparison provides information on the satellite orientation. We refer to the geomagnetic field model used this way as the *onboard model*. The second common utility of the geomagnetic field model is in the simulation of the satellite navigation system. In that case the model is used to generate the value of the Earth's magnetic field at any simulated position of the satellite. This value is in replacement of the one that would be measured by the onboard magnetometer if the satellite was effectively in orbit. The model is therefore referred to as the *simulation model*, or *truth model*.

Table 3. Contunied.

Table 3. Coefficients of the WMM2005 model. The unit of the main coefficients is in nT and the unit of the SV coefficients in nT per year for the 2005-2010 period.

n	m	g_n^m	h_n^m	\dot{g}_n^m	\dot{h}_n^m
1	0	-29556.8		8.0	
1	1	-1671.7	5079.8	10.6	-20.9
2	0	-2340.6		-15.1	
2	1	3046.9	-2594.7	-7.8	-23.2
2	2	1657.0	-516.7	-0.8	-14.6
3	0	1335.4		0.4	
3	1	-2305.1	-199.9	-2.6	5.0
3	2	1246.7	269.3	-1.2	-7.0
3	3	674.0	-524.2	-6.5	-0.6
4	0	919.8		-2.5	
4	1	798.1	281.5	2.8	2.2
4	2	211.3	-226.0	-7.0	1.6
4	3	-379.4	145.8	6.2	5.8
4	4	100.0	-304.7	-3.8	0.1
5	0	-227.4		-2.8	
5	1	354.6	42.4	0.7	0.0
5	2	208.7	179.8	-3.2	1.7
5	3	-136.5	-123.0	-1.1	2.1
5	4	-168.3	-19.5	0.1	4.8
5	5	-14.1	103.6	-0.8	-1.1
6	0	73.2		-0.7	
6	1	69.7	-20.3	0.4	-0.6
6	2	76.7	54.7	-0.3	-1.9
6	3	-151.2	63.6	2.3	-0.4
6	4	-14.9	-63.4	-2.1	-0.5
6	5	14.6	-0.1	-0.6	-0.3
6	6	-86.3	50.4	1.4	0.7
7	0	80.1		0.2	
7	1	-74.5	-61.5	-0.1	0.6
7	2	-1.4	-22.4	-0.3	0.4
7	3	38.5	7.2	1.1	0.2
7	4	12.4	25.4	0.6	0.3
7	5	9.5	11.0	0.5	-0.8
7	6	5.7	-26.4	-0.4	-0.2
7	7	1.8	-5.1	0.6	0.1
8	0	24.9		0.1	
8	1	7.7	11.2	0.3	-0.2
8	2	-11.6	-21.0	-0.4	0.1
8	3	-6.9	9.6	0.3	0.3
8	4	-18.2	-19.8	-0.3	0.4
8	5	10.0	16.1	0.2	0.1
8	6	9.2	7.7	0.4	-0.2
8	7	-11.6	-12.9	-0.7	0.4
8	8	-5.2	-0.2	0.4	0.4

n	m	g_n^m	h_n^m	\dot{g}_n^m	\dot{h}_n^m
9	0	5.6		0.0	
9	1	9.9	-20.1	0.0	0.0
9	2	3.5	12.9	0.0	0.0
9	3	-7.0	12.6	0.0	0.0
9	4	5.1	-6.7	0.0	0.0
9	5	-10.8	-8.1	0.0	0.0
9	6	-1.3	8.0	0.0	0.0
9	7	8.8	2.9	0.0	0.0
9	8	-6.7	-7.9	0.0	0.0
9	9	-9.1	6.0	0.0	0.0
10	0	-2.3		0.0	0.0
10	1	-6.3	2.4	0.0	0.0
10	2	1.6	0.2	0.0	0.0
10	3	-2.6	4.4	0.0	0.0
10	4	0.0	4.8	0.0	0.0
10	5	3.1	-6.5	0.0	0.0
10	6	0.4	-1.1	0.0	0.0
10	7	2.1	-3.4	0.0	0.0
10	8	3.9	-0.8	0.0	0.0
10	9	-0.1	-2.3	0.0	0.0
10	10	-2.3	-7.9	0.0	0.0
11	0	2.8		0.0	0.0
11	1	-1.6	0.3	0.0	0.0
11	2	-1.7	1.2	0.0	0.0
11	3	1.7	-0.8	0.0	0.0
11	4	-0.1	-2.5	0.0	0.0
11	5	0.1	0.9	0.0	0.0
11	6	-0.7	-0.6	0.0	0.0
11	7	0.7	-2.7	0.0	0.0
11	8	1.8	-0.9	0.0	0.0
11	9	0.0	-1.3	0.0	0.0
11	10	1.1	-2.0	0.0	0.0
11	11	4.1	-1.2	0.0	0.0
12	0	-2.4		0.0	0.0
12	1	-0.4	-0.4	0.0	0.0
12	2	0.2	0.3	0.0	0.0
12	3	0.8	2.4	0.0	0.0
12	4	-0.3	-2.6	0.0	0.0
12	5	1.1	0.6	0.0	0.0
12	6	-0.5	0.3	0.0	0.0
12	7	0.4	0.0	0.0	0.0
12	8	-0.3	0.0	0.0	0.0
12	9	-0.3	0.3	0.0	0.0
12	10	-0.1	-0.9	0.0	0.0
12	11	-0.3	-0.4	0.0	0.0
12	12	-0.1	0.8	0.0	0.0

With a recursive algorithm implementing Eq. (5) in Matlab® it was possible to generate the value of the geomagnetic field for any given orbit at the desired epoch. It is this algorithm that is used for the onboard model and for the simulation model. The geomagnetic field vector is represented in Figure 3

along a circular orbit of altitude 540 km, inclined 2 degrees, at the epoch 2005.16 years (equivalent to 1st March 2005). Its components in the *Geocentric Equatorial* coordinate system and its magnitude are plotted in Figure 4.

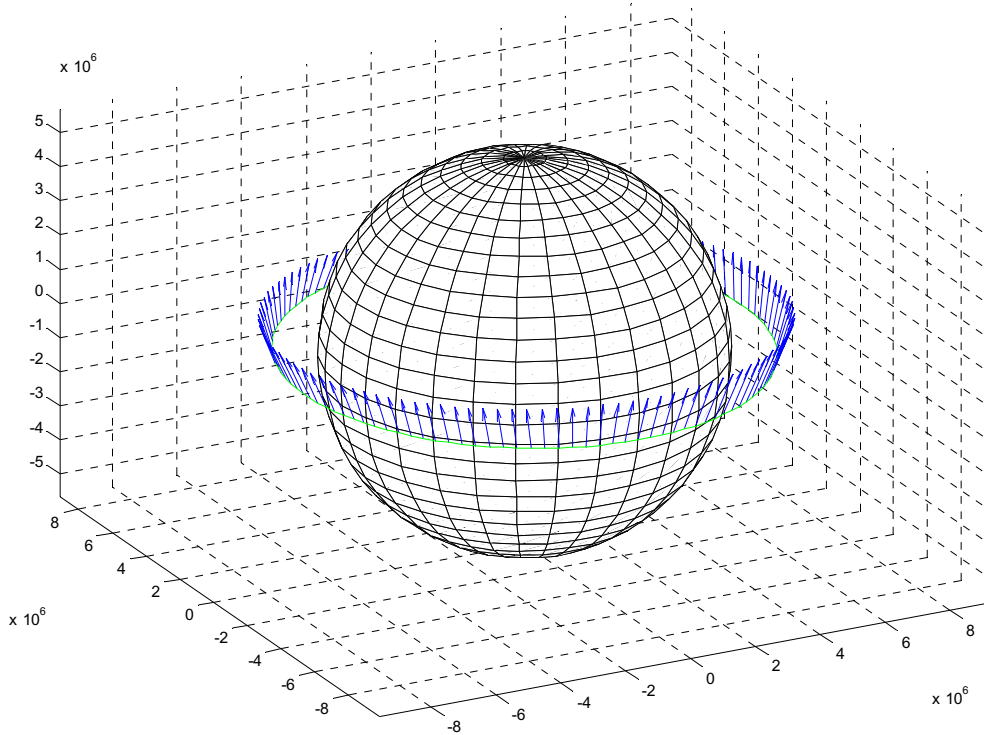


Figure 3. Earth's magnetic field vector along a circular orbit inclined 2 degrees.

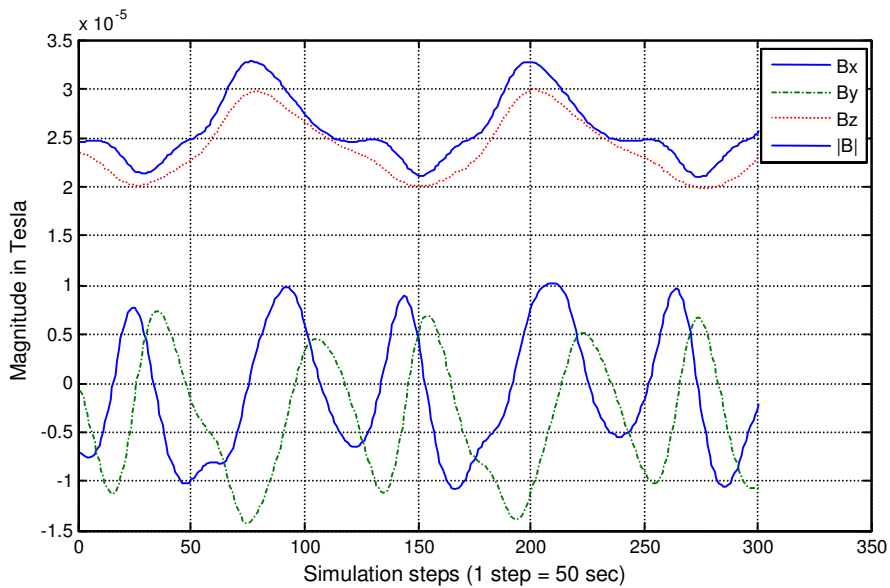


Figure 4. Earth's magnetic field components along a circular orbit inclined 2 degrees.

As can be seen in Table 3, the maximum degree of the WMM2005 model is $n = 12$. The maximum accuracy in the estimation of the geomagnetic field is obtained for this degree, meaning that all the Gauss coefficients are accounted for in the algorithm used to generate the field. The following section provides a comparison of the accuracy of the WMM2005 model when different modeling degrees are used. This analysis is useful for determining the optimal degree re-

quired by the satellite's onboard magnetic model. The smaller the degree used for the model the faster the computation is realized by the microprocessor. It is common on many CubeSat¹ satellites (where the processing capacities are greatly limited) to truncate the model to the degree 6, as in spite of the modeling error created by this approximation the satellite still meets the requirements of the mission (Giesselmann, 2004).

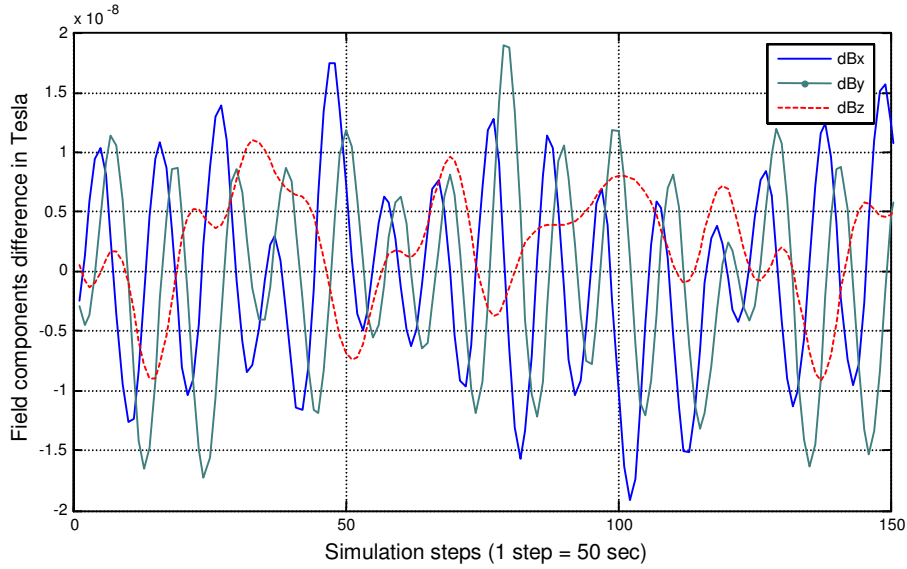


Figure 5. Field components differences for the WMM2005 model between degree 12 and degree 10, along a circular orbit inclined 2 degrees of altitude 540 km.

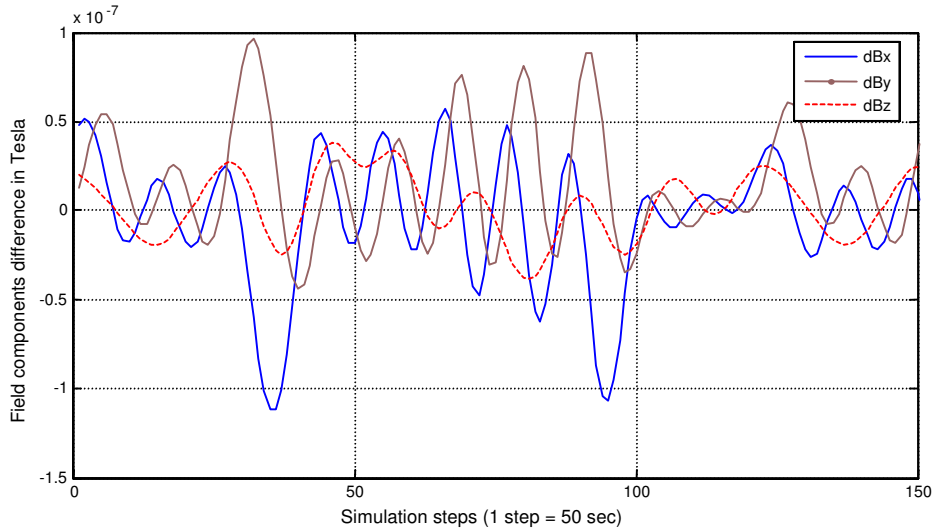


Figure 6. Field components differences for the WMM2005 model between degree 12 and degree 8, along a circular orbit inclined 2 degrees of altitude 540 km.

¹A CubeSat is a standardized satellite of cubic shape with length of 10 cm and maximum weight of 1 kg.

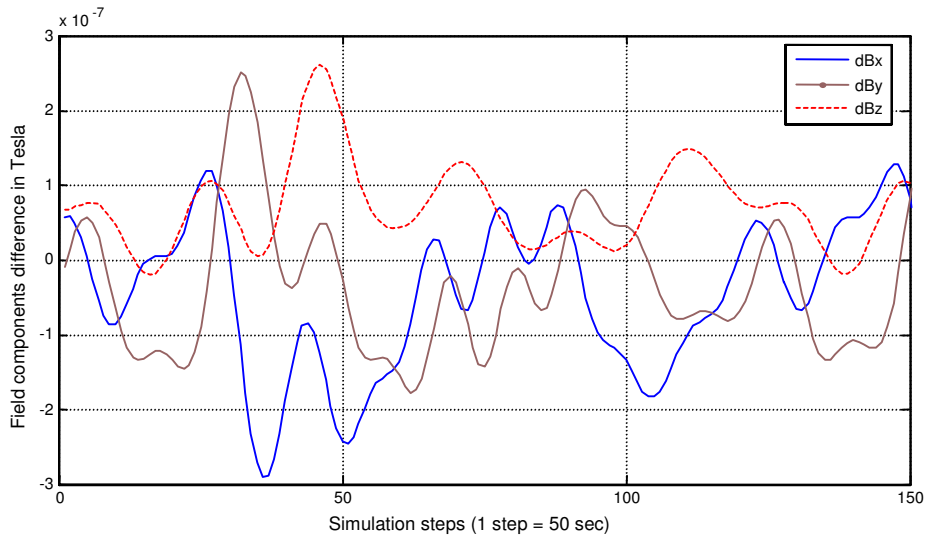


Figure 7. Field components differences for the WMM2005 model between degree 12 and degree 6, along a circular orbit inclined 2 degrees of altitude 540 km.

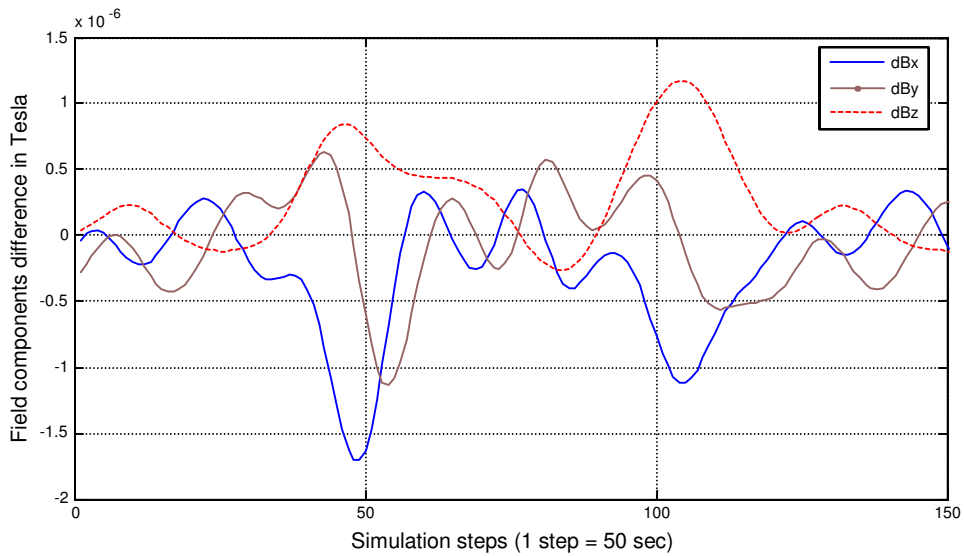


Figure 8. Field components differences for the WMM2005 model between degree 12 and degree 4, along a circular orbit inclined 2 degrees of altitude 540 km.

If we assume that the model of degree 12 represents reality, the plots of the difference between this model and models of lower degree indicate the error realized on each component of the geomagnetic field. Figures 5 to 8 show that the error on each component of the geomagnetic field increases as well as the standard deviation for each component (Figure 9).

This level of accuracy is usually satisfactory for

most nanosatellite missions as the magnetometer sensor will be subjected to disturbance fields due to magnetic materials and electric currents in the satellite electronics that are also in this order of magnitude. If we choose the model of degree 6, the error will be less than 1.4%, and for the model of degree 4 the error will be less than 5.6%.

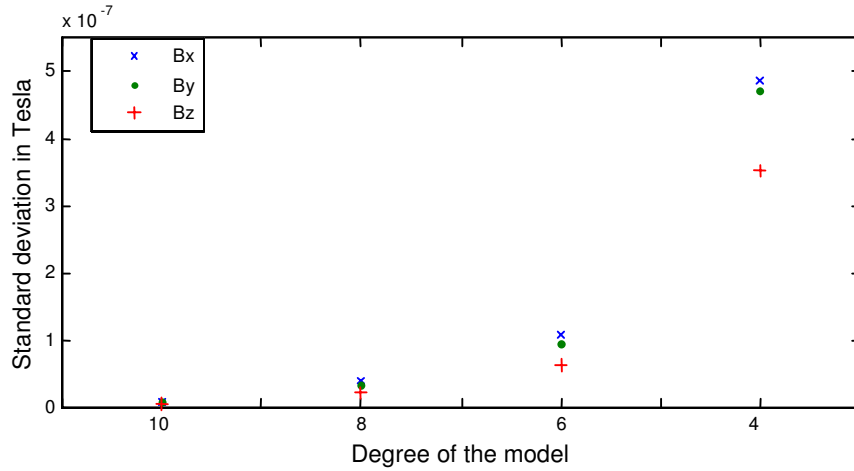


Figure 9. Standard deviation for each component as a function of the degree of the model.

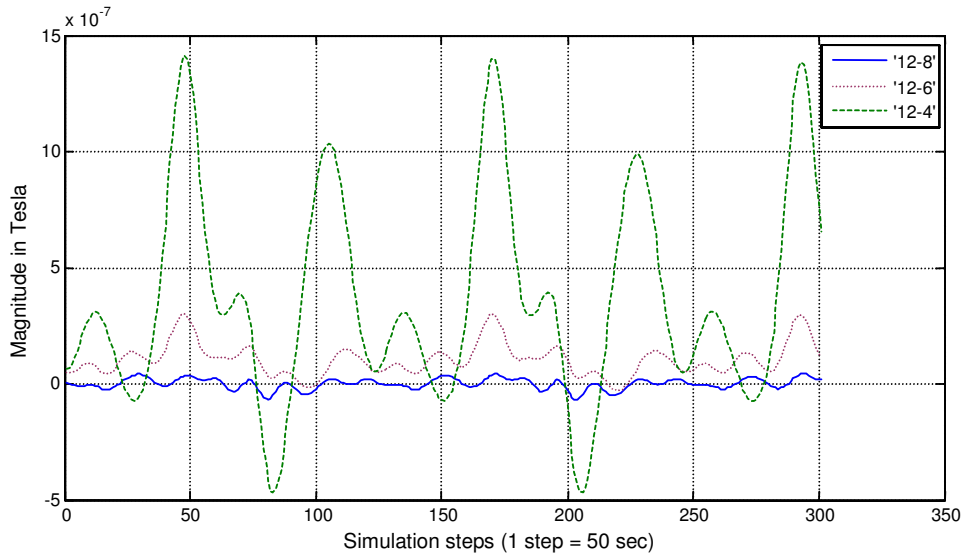


Figure 10. Field magnitude for the differences between model 12 and 8, 12 and 6, and 12 and 4, using the WMM2005 model along a circular orbit inclined 2 degrees.

Considering that the geomagnetic field amplitude for the circular orbit considered in Figure 4 is varying between 20,000 and 35,000 nT, the error created on the geomagnetic field amplitude by using a model truncated to the degree 8 will be less than 0.3% , and will stay in the interval ± 100 nT (Figure 10).

Magnetometer for Space Applicatons

Space magnetometers are simple, reliable and widely available for under USD 10,000. Magnetometers used to measure the Earth’s magnetic field are mainly of 3 different types: fluxgate, magnetoinductive and anisotropic magnetoresistive (AMR). Flux-

gate magnetometers are the most common type used for navigation. Based on a primary coil excited at a constant frequency and a secondary coil that output a signal coupled to the drive voltage through the ferromagnetic core of the sensor. The voltage at the secondary coil is sensitive to any variation of the external magnetic field. The 3-axis fluxgate magnetometer designed by *Surrey Satellite Technology Ltd* has a range of $\pm 60 \mu\text{T}$ with a very low power consumption of 0.147 W. The operating temperature is between -50 and $+80 \text{ }^\circ\text{C}$, which is sufficient to withstand the temperature variation of the space environment (Figure 11).

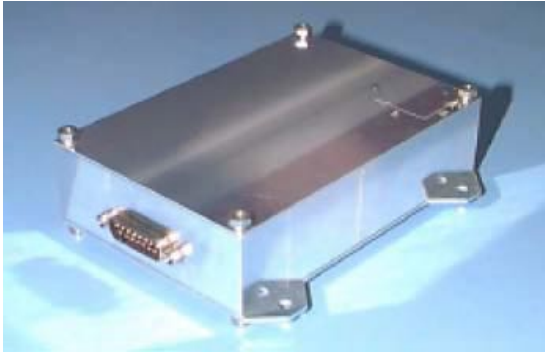


Figure 11. Fluxgate Magnetometer (130 x 90 x 36 mm, 295 g) from *Surrey Satellite Technology*.

The magnetoinductive sensor is relatively new, with the first patent issued in 1989. It has the advantages of being cheaper and smaller than the fluxgate sensor. The TCM2 magnetometer manufactured by *Precision Navigation Inc.* has a resolution of 10 nT, a range of $\pm 80 \mu\text{T}$ and an operating temperature between -20 and $+70 \text{ }^\circ\text{C}$. Its dimensions are 63.5 x 50.8 x 31.75 mm and weight is 45.5 g. The power consumption is less than 0.12 W.

The AMR magnetometer has the widest range of application: disk drive heads, wheel speed sensing, current sensing, compass navigation and satellite attitude determination.

Honeywell manufactures a variety of magnetic sensors based on the property of a permalloy film to change in resistance in the presence of a magnetic field. The HMR2300 has been used in the Canadian nanosat CanX-1 launched on June 30 2003 and the NCUBE1 and NCUBE2 nanosatellites from NTN University in Norway (launch date planned for the first half of 2005). The characteristics of the HMR2300 are as follows: range of $\pm 200 \mu\text{T}$, resolution of 6.7 nT and operating temperature from -40 and $+85 \text{ }^\circ\text{C}$. The magnetometer board weighs 28 g

and measures 74.9 x 30.5 x 22 mm, while consuming a maximum power of 0.228 W.

The HMC2003 has been used in the following missions already: HokieSat from Virginia Tech University (never launched), TU-Sat-1 from Taylor University launched on May 2002 and Dawgstar from University of Washington (launched in the beginning of 2003). The HMC1001 and HMC1002 have been used in the CubeSat from Aalborg University in Sweden (launched on June 2003). These 2 sensors are also the primary components of the HMR2300 and are used to measure the magnetic field along 1 and 2 axes, respectively. The HMC1021 has been used in the DTUSat of the Technical University of Denmark (launched on June 2003). It is a one-axis sensor. The HMC1022 is the equivalent 2-axis sensor.

According to Svartveit (2003), based on the attitude determination design of the NCUBE nanosatellite, it seems that a digital magnetometer, like the HMR2300, priced at approximately USD 700, is preferred to analog output magnetometer like the HMC2003, which is about 3 times less expensive. The features of the *Honeywell* magnetoresistive sensors are summarized in Table 4.

Attitude Determination

The attitude of a satellite or any solid object is defined as its orientation in space. To evaluate this orientation we need to have a system of references from which we can compare the satellite's present orientation with a past, or initial, orientation. This system is defined in terms of reference frames: the geocentric reference frame (GRF), for which the fundamental plane is the Earth's equatorial plane and the principal axis is the line pointing from the center

Table 4. Comparison of *Honeywell* magnetoresistive sensors' characteristics.

	Resolution (nT)	Range (μT)	Temperature sensitivity (ppm/ $^\circ\text{C}$)	Weight (g)	Dimensions (mm)	Output	Axis
HMC1001	2.7	± 200	- 3000	0.14	(11 x 7 x 1.5)*	Analog	1
HMC1021	8.5	± 600	- 3000	NA	(6 x 4.9 x 1.5)*	Analog	1
HMC2003	4.0	± 200	- 600	NA	25.9 x 18.0 x 10.9	Analog	3
HMR2300	6.7	± 200	- 600	28	74.9 x 30.5 x (20)*	Digital	3

* Dimensions in parentheses are approximate.

of the Earth toward the vernal equinox, and the satellite reference frame (SRF) that is fixed with respect to the satellite body. The relative orientation of the satellite reference frame with the geocentric reference frame provides a representation of the satellite attitude. There exist different ways to parameterize this attitude: rotation matrix, Euler angles, Rodriguez parameters, quaternions, etc.

The determination process of the attitude starts from the sensors onboard the satellite that will provide a measurement of some reference vectors with respect to the SRF, like the direction of the Sun, the direction of the Earth's center, the direction of the geomagnetic field or the direction of some particular stars. For our mission only the magnetometer onboard will provide data to the determination algorithm (Figure 12). The rate of rotation of the satellite, whose knowledge is particularly useful in various control modes like detumbling or slew maneuvers, can be inertially measured by a gyroscope. These measured directions are then compared with predicted values defined in the GRF. The prediction process, realized onboard the satellite, requires the knowledge of the satellite position in its orbit, obtained from an orbit propagation model and the time since this model was updated. It is the way of processing these data (measured and predicted vectors) that constitutes the specificity of the attitude determination algorithm.

There are 2 main categories of algorithms, namely deterministic methods and statistical methods. The former category, also called single-point methods, are based on 2 vector observations at a single time point.

Among these methods we can make a distinction

between optimal and non-optimal algorithms. The Cones Intersection technique (Grubin, 1977) and the TRIAD algorithm (Lerner, 1978) are the first non-optimal deterministic methods that have been discussed in the literature. They are simple to implement but lack accuracy as they assume perfect measurement of the reference vectors, which is never realized.

The optimal solution is such that the error inherent to the measurement process, a priori different for each sensor, is minimized. Among the most popular optimal solutions used in real applications are the QUEST algorithm described in Shuster and Oh (1981), the SVD method from Markley (1988), the FOAM method from Markley (1993), and the ESOQ1 and ESOQ2 methods from Mortari (1997a, 1997b).

The previous methods, although providing efficient algorithms, suffer from a number of shortcomings considering our particular mission. First of all they require the simultaneous measurement of at least 2 reference vectors, which is clearly not possible if we use only a magnetometer. Secondly they require the measurement of the satellite rate of rotation, whereas for a low-cost mission it is usually preferred to use a gyroless configuration for reasons like power consumption and the high cost of an accurate gyro.

Statistical, or recursive, methods are also considered optimal as the solution (the attitude matrix) must minimize a cost function. They are mainly based on the theory of Kalman filtering (Kalman, 1960) and their differences from deterministic methods are in the use of the following information in the estimation process:

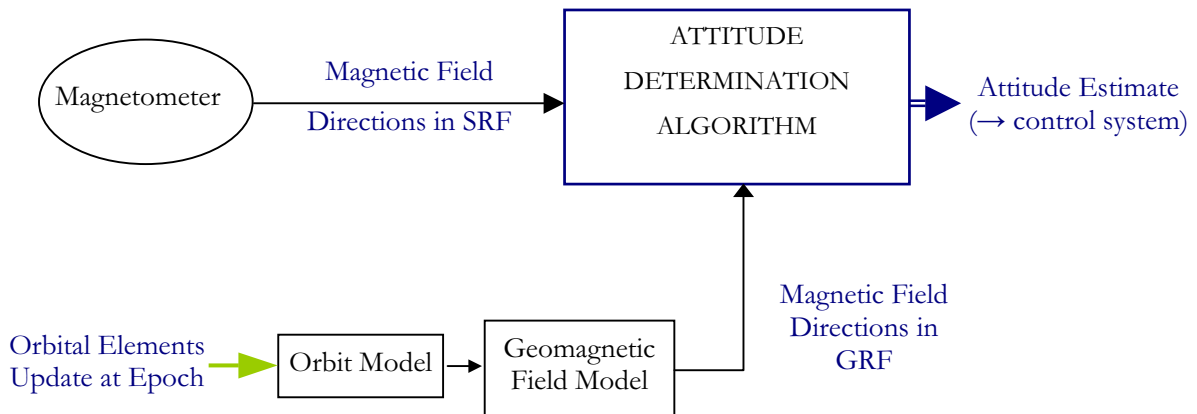


Figure 12. Conceptual diagram of the nanosat attitude estimation process.

- the dynamics of the satellite and attitude sensors,
- the consideration of the measurement errors, system noises and uncertainty in the dynamics models,
- the use of all available measuring devices, which leads to an over-determined problem.

A review covering the first 20 years of Kalman filtering methods applied to the attitude estimation is available in Lefferts et al. (1982). One of the main problems of Kalman filtering is the need for accurate models of the satellite, the sensors, and the different sources of noise. If we want to estimate the state $x \in \mathbb{R}^n$ of the system, where the vector x contains the information required to determine the satellite attitude, we can represent the problem using the following discrete equations:

$$x_k = Ax_{k-1} + Bu_k + w_{k-1}, \quad (8)$$

$$z_k = Hx_k + v_k. \quad (9)$$

The vector $z \in \mathbb{R}^m$ represents a measurement of the state and $u \in \mathbb{R}^l$ is an optional control input. The process and measurement noise are respectively represented by the random variables w_k and v_k , assumed to be independent, Gaussian, with zero mean:

$$p(w) \sim N(0, Q), \quad (10)$$

$$p(v) \sim N(0, R). \quad (11)$$

The matrices Q and R are the covariance for the process noise and the measurement noise, respectively. They are assumed to be known and constant, whereas in practice they can change at each time step. The matrices A , B and H are also assumed to be constant. The goal of the Kalman filter is then to provide the best estimate of the state vector so that we can derive the satellite attitude. A possible value for x would be

$$x = \begin{bmatrix} q_1 \\ q_2 \\ q_3 \\ q_4 \\ \omega_x \\ \omega_y \\ \omega_z \end{bmatrix} \quad (12)$$

where the first 4 coordinates represent the quaternion vector and the last 3 coordinates stand for the rate of rotation of the satellite. The filter should be first initialized with an initial state vector \hat{x}_0 (the hat indicates that it is an estimate) and an associated covariance matrix. The recursive operation starts with a prediction stage where an a priori state estimate, \hat{x}_k^- , is found based on the process model and \hat{x}_0 (if $k=1$) or \hat{x}_{k-1}^- (for any $k > 1$). The update stage follow and gives the a posteriori estimate of the state, \hat{x}_k^+ , based on the measurement z_k made at time t_k . The operation continues with the prediction of \hat{x}_{k+1}^- using \hat{x}_k^+ .

Figure 13 shows the flow of the estimation process.

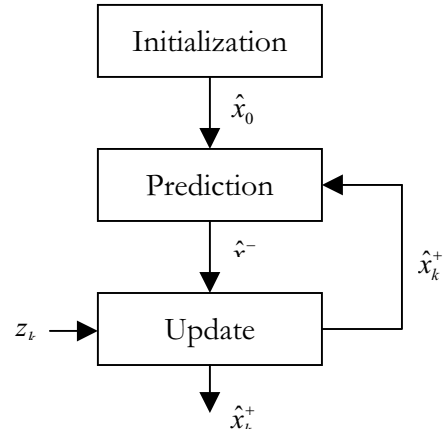


Figure 13. Kalman filter operation flow.

One of the main drawbacks of the Kalman filtering technique is that it requires the assumption that white noises follow a Gaussian law. This restriction is overcome with the Minimum Model Error (MME) estimator introduced by Mook and Junkins (1988), where the model error and the state vector are estimated simultaneously. The inconvenience of this algorithm is that it is off-line and must utilize post-experiment measurements. Crassidis and Markley (1997) developed an on-line equivalent of the MME estimator specifically for a gyroless satellite.

Conclusion

After mentioning the specificities of nanosatellites and justifying their relevance with respect to other types of satellite, we described the main source of reference used to determine the satellite attitude: the Earth's magnetic field. The existing types of COST

magnetometers and their usage in nanosatellite are presented. The attitude determination process is briefly explained along with the 2 main categories of attitude determination algorithms. The Kalman filtering technique, which is extensively utilized in the design of navigation systems, is also presented.

References

- Campbell, W.H., Introduction to Geomagnetic Fields, 2nd ed. Cambridge Univ. Press, 2003.
- Crassidis, J.L. and Markley, F.L., "Predictive Filtering for Attitude Estimation without Rate Sensors," Journal of Guidance, Control and Dynamics, 20, 522-527, 1997.
- Giesselmann, J., "Compass One: International Geomagnetic Reference Field 2000", Technical Note 420-04, University of Applied Sciences, Aachen, Germany, 2004.
- Grubin, C., "Simple Algorithm for Intersecting Two Conical Surfaces", Journal of Spacecraft and Rockets, 14, 251-252, 1977.
- Kalman, R.E., "A New Approach to Linear Filtering and Prediction Problems", Transactions of ASME, series D, Journal of Basic Engineering 82, 35-45, 1960.
- Lefferts, E.J., Markley, F.L. and Shuster, M.D., "Kalman Filtering for Spacecraft Attitude Estimation", Journal of Guidance, Control, and Dynamics, 5, 417-429, 1982.
- Lerner, G.M., "Spacecraft Attitude Determination and Control", Kluwer Academic, 420-428, 1978.
- Macmillan, S., Private Communications, Geomagnetism Group, British Geological Survey, UK, 2005.
- Markley, F.L., "Attitude Determination Using Vector Observations and the Singular Value Decomposition", The Journal of the Astronautical Sciences, 36, 245-258, 1988.
- Markley, F.L., "Attitude Determination from Vector Observations: A Fast Optimal Matrix Algorithm", The Journal of the Astronautical Sciences, 41, 261-280, 1993.
- Mook, D.J. and Junkins, J.L., "Minimum Model Error Estimation for Poorly Modeled Dynamic Systems", Journal of Guidance, Control and Dynamics, 3, 367-375, 1988.
- Mortari, D., "ESOQ: A Closed-Form Solution to the Wahba Problem", Journal of the Astronautical Sciences, 45, 195-204, 1997a.
- Mortari, D., "ESOQ-2 Single-Point Algorithm for Fast Optimal Spacecraft Attitude Determination", Advances in the Astronautical Sciences, Vol. 95, Pt. II, 817-826, 7th Annual AIAA/AAS Space Flight Mechanics Meeting, Huntsville, AL, Feb. 10-12, 1997b.
- Olsen, N., "A Model of the Geomagnetic Field and its Secular Variation for Epoch 2000 Estimated from Ørsted Data", Geophys. J. Int., 149, 454-462, 2002.
- Shuster, M. and Oh, S., "Three-Axis Attitude Determination from Vector Observations", Journal of Guidance and Control, 4, 70-77, 1981.